# Evidential Neural Radiance Fields

## Supplementary Material

## 8. Derivations: Point-to-Pixel Propagation of Radiance and Uncertainty

This section derives the propagation formulae of radiance and uncertainties specified in Equations (12) and (13).

The mean color aggregation formula follows directly from the linearity of expectation, which does not require any independence assumption.

$$\bar{c} = \mathbb{E}[c] = \mathbb{E}\left[\sum_{i=1}^{N} w_i c_i\right] = \sum_{i=1}^{N} w_i \mathbb{E}[c_i] = \sum_{i=1}^{N} w_i \bar{c}_i. \tag{26}$$

Deriving the three uncertainty propagation formulae each requires its own independence assumption. However, only two, and any two, of these three assumptions are necessary to derive all the three formulae.

**Assumption 1.** *The point colors are independent, i.e.,* $c_i \perp\!\!\!\perp c_j,\ \forall i \neq j$.

**Assumption 2.** *The point colors are conditionally independent given the conditional means and variances, i.e.,* $c_i \perp\!\!\!\perp c_j \mid \boldsymbol{\theta},\ \forall i \neq j$.

**Assumption 3.** *The point colors' conditional means are independent, i.e.,* $\mu_i \perp\!\!\!\perp \mu_j,\ \forall i \neq j$.

With these assumptions, it can be shown that

$$U = \mathrm{Var}[c] = \mathrm{Var}\left[\sum_{i=1}^{N} w_i c_i\right] \overset{\text{A.1}}{=} \sum_{i=1}^{N} w_i^2 \mathrm{Var}[c_i] = \sum_{i=1}^{N} w_i^2 U_i, \tag{27}$$

$$\begin{aligned} U^{\text{alea}} &= \mathbb{E}[\mathrm{Var}[c \,|\, \boldsymbol{\theta}]] = \mathbb{E}\left[\mathrm{Var}\left[\sum_{i=1}^{N} w_i c_i \,\middle|\, \boldsymbol{\theta}\right]\right] \overset{\text{A.2}}{=} \mathbb{E}\left[\sum_{i=1}^{N} w_i^2 \mathrm{Var}[c_i \,|\, \boldsymbol{\theta}]\right] \\ &= \sum_{i=1}^{N} w_i^2 \mathbb{E}\left[\mathrm{Var}[c_i \,|\, \boldsymbol{\theta}]\right] = \sum_{i=1}^{N} w_i^2 \mathbb{E}\left[\mathrm{Var}[c_i \,|\, \mu_i, \sigma_i^2]\right] = \sum_{i=1}^{N} w_i^2 U_i^{\text{alea}}, \end{aligned} \tag{28}$$

$$\begin{aligned} U^{\text{epis}} &= \mathrm{Var}[\mathbb{E}[c \,|\, \boldsymbol{\theta}]] = \mathrm{Var}\left[\mathbb{E}\left[\sum_{i=1}^{N} w_i c_i \,\middle|\, \boldsymbol{\theta}\right]\right] = \mathrm{Var}\left[\sum_{i=1}^{N} w_i \mathbb{E}[c_i \,|\, \boldsymbol{\theta}]\right] \\ &\overset{\text{A.3}}{=} \sum_{i=1}^{N} w_i^2 \mathrm{Var}\left[\mathbb{E}[c_i \,|\, \boldsymbol{\theta}]\right] = \sum_{i=1}^{N} w_i^2 \mathrm{Var}[\mathbb{E}[c_i \,|\, \mu_i, \sigma_i^2]] = \sum_{i=1}^{N} w_i^2 U_i^{\text{epis}}, \end{aligned} \tag{29}$$

where $\overset{\text{A.}n}{=}$ denotes the step where Assumption $n$ is used.

These three equations are connected by the law of total variance, as

$$\underbrace{\mathrm{Var}[c]}_{U} = \underbrace{\mathbb{E}[\mathrm{Var}[c \,|\, \boldsymbol{\theta}]]}_{U^{\text{alea}}} + \underbrace{\mathrm{Var}[\mathbb{E}[c \,|\, \boldsymbol{\theta}]]}_{U^{\text{epis}}}, \tag{30}$$

$$\underbrace{\mathrm{Var}[c_i]}_{U_i} = \underbrace{\mathbb{E}[\mathrm{Var}[c_i \,|\, \mu_i, \sigma_i^2]]}_{U_i^{\text{alea}}} + \underbrace{\mathrm{Var}[\mathbb{E}[c_i \,|\, \mu_i, \sigma_i^2]]}_{U_i^{\text{epis}}}. \tag{31}$$

Therefore, any two of Equations (27) to (29) imply the third, and thus only two of Assumptions 1 to 3 are necessary to derive all the three equations.

# 9. Derivations: Pixel Radiance Marginal Distribution and Loss Function

This section derives the marginal distribution of pixel radiance and the negative log-likelihood loss in Equations (21) and (23).

Evidential NeRF defines each pixel radiance $c$ by a hierarchical probabilistic model

$$c \mid \mu, \sigma^2 \sim \mathcal{N}(\mu, \sigma^2), \qquad \mu \mid \sigma^2 \sim \mathcal{N}(\gamma, \sigma^2/\nu), \qquad \sigma^2 \sim \Gamma^{-1}(\alpha, \beta), \tag{32}$$

where $\mathcal{N}(\cdot,\cdot)$ and $\Gamma^{-1}(\cdot,\cdot)$ respectively denote normal distribution and inverse-gamma distribution and $\gamma \in \mathbb{R}$, $\nu > 0$, $\alpha > 1$, and $\beta > 0$ are the evidential NIG parameters. Based on these prerequisites, we derive the marginal distribution and negative log-likelihood of the pixel color $c$.

The probability density functions of the distributions in Equation (32) are respectively given by

$$p(c \mid \mu, \sigma^2) = \frac{1}{\sqrt{2\pi\sigma^2}} \exp\left(-\frac{(c-\mu)^2}{2\sigma^2}\right), \tag{33}$$

$$p(\mu \mid \sigma^2) = \frac{\sqrt{\nu}}{\sqrt{2\pi\sigma^2}} \exp\left(-\frac{(\mu-\gamma)^2\nu}{2\sigma^2}\right), \tag{34}$$

$$p(\sigma^2) = \frac{\beta^\alpha}{\Gamma(\alpha)} (\sigma^2)^{-\alpha-1} \exp\left(-\frac{\beta}{\sigma^2}\right). \tag{35}$$

It can therefore be shown that

$$p(c \mid \sigma^2) \tag{36}$$

$$= \int_{-\infty}^{\infty} p(c \mid \mu, \sigma^2) p(\mu \mid \sigma^2) d\mu \tag{37}$$

$$= \int_{-\infty}^{\infty} \frac{1}{\sqrt{2\pi\sigma^2}} \exp\left(-\frac{(c-\mu)^2}{2\sigma^2}\right) \frac{\sqrt{\nu}}{\sqrt{2\pi\sigma^2}} \exp\left(-\frac{(\mu-\gamma)^2\nu}{2\sigma^2}\right) d\mu \tag{38}$$

$$= \int_{-\infty}^{\infty} \frac{\sqrt{\nu}}{2\pi\sigma^2} \exp\left(-\frac{(c-\mu)^2 + (\mu-\gamma)^2\nu}{2\sigma^2}\right) d\mu \tag{39}$$

$$= \int_{-\infty}^{\infty} \frac{\sqrt{\nu}}{2\pi\sigma^2} \exp\left(-\frac{(\nu+1)\mu^2 - 2(c+\gamma\nu)\mu + (c^2+\gamma^2\nu)}{2\sigma^2}\right) d\mu \tag{40}$$

$$= \frac{\sqrt{\nu}}{2\pi\sigma^2} \exp\left(-\frac{c^2+\gamma^2\nu}{2\sigma^2}\right) \int_{-\infty}^{\infty} \exp\left(-\frac{(\nu+1)\mu^2 - 2(c+\gamma\nu)\mu}{2\sigma^2}\right) d\mu \tag{41}$$

$$= \frac{\sqrt{\nu}}{2\pi\sigma^2} \exp\left(-\frac{c^2+\gamma^2\nu}{2\sigma^2}\right) \int_{-\infty}^{\infty} \exp\left(-\frac{(\mu - \frac{c+\gamma\nu}{\nu+1})^2 - (\frac{c+\gamma\nu}{\nu+1})^2}{\frac{2\sigma^2}{\nu+1}}\right) d\mu \tag{42}$$

$$= \frac{\sqrt{\nu}}{2\pi\sigma^2} \exp\left(-\frac{c^2+\gamma^2\nu}{2\sigma^2}\right) \exp\left(\frac{(c+\gamma\nu)^2}{2\sigma^2(\nu+1)}\right) \int_{-\infty}^{\infty} \exp\left(-\frac{(\mu - \frac{c+\gamma\nu}{\nu+1})^2}{\frac{2\sigma^2}{\nu+1}}\right) d\mu \tag{43}$$

$$= \frac{\sqrt{\nu}}{2\pi\sigma^2} \exp\left(-\frac{c^2+\gamma^2\nu}{2\sigma^2} + \frac{(c+\gamma\nu)^2}{2\sigma^2(\nu+1)}\right) \int_{-\infty}^{\infty} \sqrt{2\pi\frac{\sigma^2}{\nu+1}} \mathcal{N}\left(\mu; \frac{c+\gamma\nu}{\nu+1}, \frac{\sigma^2}{\nu+1}\right) d\mu \tag{44}$$

$$= \frac{\sqrt{\nu}}{2\pi\sigma^2} \sqrt{2\pi\frac{\sigma^2}{\nu+1}} \exp\left(-\frac{(c^2+\gamma^2\nu)(\nu+1) - (c+\gamma\nu)^2}{2\sigma^2(\nu+1)}\right) \int_{-\infty}^{\infty} \mathcal{N}\left(\mu; \frac{c+\gamma\nu}{\nu+1}, \frac{\sigma^2}{\nu+1}\right) d\mu \tag{45}$$

$$= \frac{\sqrt{\nu}}{2\pi\sigma^2} \sqrt{2\pi\frac{\sigma^2}{\nu+1}} \exp\left(-\frac{(c^2+\gamma^2\nu)(\nu+1) - (c+\gamma\nu)^2}{2\sigma^2(\nu+1)}\right) \tag{46}$$

$$= \sqrt{\frac{\nu}{2\pi\sigma^2(\nu+1)}} \exp\left(-\frac{(c-\gamma)^2\nu}{2\sigma^2(\nu+1)}\right), \tag{47}$$

i.e.,

$$c \mid \sigma^2 \sim \mathcal{N}\left(\gamma, \frac{\sigma^2(\nu+1)}{\nu}\right), \tag{48}$$

and thus,

$$
\begin{aligned}
& p(c) && (49)\\
&= \int_0^\infty p(c \mid \sigma^2) p(\sigma^2) d\sigma^2 && (50)\\
&= \int_0^\infty \sqrt{\frac{\nu}{2\pi\sigma^2(\nu+1)}} \exp\left(-\frac{(c-\gamma)^2\nu}{2\sigma^2(\nu+1)}\right) \frac{\beta^\alpha}{\Gamma(\alpha)} (\sigma^2)^{-\alpha-1} \exp\left(-\frac{\beta}{\sigma^2}\right) d\sigma^2 && (51)\\
&= \sqrt{\frac{\nu}{2\pi(\nu+1)}} \frac{\beta^\alpha}{\Gamma(\alpha)} \int_0^\infty \exp\left(-\frac{(c-\gamma)^2\nu}{2\sigma^2(\nu+1)} - \frac{\beta}{\sigma^2}\right) (\sigma^2)^{-\alpha-\frac{3}{2}} d\sigma^2 && (52)\\
&= \sqrt{\frac{\nu}{2\pi(\nu+1)}} \frac{\beta^\alpha}{\Gamma(\alpha)} \int_0^\infty \exp\left(-\frac{\frac{(c-\gamma)^2\nu}{2(\nu+1)} + \beta}{\sigma^2}\right) (\sigma^2)^{-\alpha-\frac{3}{2}} d\sigma^2 && (53)\\
&= \sqrt{\frac{\nu}{2\pi(\nu+1)}} \frac{\beta^\alpha}{\Gamma(\alpha)} \int_0^\infty \frac{\Gamma\left(\alpha+\frac{1}{2}\right)}{\left(\frac{(c-\gamma)^2\nu}{2(\nu+1)} + \beta\right)^{\alpha+\frac{1}{2}}} \Gamma^{-1}\left(\sigma^2; \alpha+\frac{1}{2}, \frac{(c-\gamma)^2\nu}{2(\nu+1)} + \beta\right) d\sigma^2 && (54)\\
&= \sqrt{\frac{\nu}{2\pi(\nu+1)}} \frac{\beta^\alpha}{\Gamma(\alpha)} \frac{\Gamma\left(\alpha+\frac{1}{2}\right)}{\left(\frac{(c-\gamma)^2\nu}{2(\nu+1)} + \beta\right)^{\alpha+\frac{1}{2}}} \int_0^\infty \Gamma^{-1}\left(\sigma^2; \alpha+\frac{1}{2}, \frac{(c-\gamma)^2\nu}{2(\nu+1)} + \beta\right) d\sigma^2 && (55)\\
&= \sqrt{\frac{\nu}{2\pi(\nu+1)}} \frac{\beta^\alpha}{\Gamma(\alpha)} \frac{\Gamma\left(\alpha+\frac{1}{2}\right)}{\left(\frac{(c-\gamma)^2\nu}{2(\nu+1)} + \beta\right)^{\alpha+\frac{1}{2}}} && (56)\\
&= \frac{\Gamma\left(\alpha+\frac{1}{2}\right)}{\Gamma(\alpha)\sqrt{2\pi\frac{\beta(\nu+1)}{\nu}}} \left(\frac{(c-\gamma)^2}{2\frac{\beta(\nu+1)}{\nu}} + 1\right)^{-\left(\alpha+\frac{1}{2}\right)} && (57)\\
&= \frac{\Gamma(\frac{\nu_t+1}{2})}{\Gamma(\frac{\nu_t}{2})\sqrt{\pi\nu_t\sigma_t^2}} \left(\frac{(c-\mu_t)^2}{\nu_t\sigma_t^2} + 1\right)^{-\frac{\nu_t+1}{2}}, && (58)
\end{aligned}
$$

i.e.,

$$
c \sim t\left(\mu_t = \gamma, \sigma_t^2 = \frac{\beta(\nu+1)}{\alpha\nu}, \nu_t = 2\alpha\right), \tag{59}
$$

where $t(\mu_t, \sigma_t^2, \nu_t)$ denotes a Student's $t$ distribution with location $\mu_t$, scale $\sigma_t$, and degrees of freedom $\nu_t$, and $\mathcal{N}(x; \cdot, \cdot)$ and $\Gamma^{-1}(x; \cdot, \cdot)$ represent their probability distribution densities at $x$. This yields Equation (21).

The negative log-likelihood of $c$ can thereby be derived as

$$
\begin{aligned}
& -\log p(c) && (60)\\
&= -\log\left(\frac{\Gamma\left(\alpha+\frac{1}{2}\right)}{\Gamma(\alpha)\sqrt{2\pi\frac{\beta(\nu+1)}{\nu}}} \left(\frac{(c-\gamma)^2}{2\frac{\beta(\nu+1)}{\nu}} + 1\right)^{-\left(\alpha+\frac{1}{2}\right)}\right) && (61)\\
&= \frac{1}{2}\log\left(2\pi\frac{\beta(\nu+1)}{\nu}\right) + \log\frac{\Gamma(\alpha)}{\Gamma\left(\alpha+\frac{1}{2}\right)} + \left(\alpha+\frac{1}{2}\right)\log\left(\frac{(c-\gamma)^2}{2\frac{\beta(\nu+1)}{\nu}} + 1\right) && (62)\\
&= \frac{1}{2}\log\frac{\pi}{\nu} + \frac{1}{2}\log\left(2\beta(\nu+1)\right) + \log\frac{\Gamma(\alpha)}{\Gamma\left(\alpha+\frac{1}{2}\right)} + \left(\alpha+\frac{1}{2}\right)\log\left(\frac{(c-\gamma)^2\nu}{2\beta(\nu+1)} + 1\right) && (63)\\
&= \frac{1}{2}\log\frac{\pi}{\nu} - \alpha\log\left(2\beta(\nu+1)\right) + \log\frac{\Gamma(\alpha)}{\Gamma\left(\alpha+\frac{1}{2}\right)} + \left(\alpha+\frac{1}{2}\right)\log\left((c-\gamma)^2\nu + 2\beta(\nu+1)\right) && (64)\\
&= \frac{1}{2}\log\frac{\pi}{\nu} - \alpha\log\Omega + \log\frac{\Gamma(\alpha)}{\Gamma\left(\alpha+\frac{1}{2}\right)} + \left(\alpha+\frac{1}{2}\right)\log\left((c-\gamma)^2\nu + \Omega\right), && (65)
\end{aligned}
$$

where $\Omega = 2\beta(1+\nu)$. This yields Equation (23).

# 10. Further Discussions

**More quantitative results.** In the main paper, quantitative results averaged across all scenes within each dataset are reported. Tables 4 to 7 provide per-scene statistics including the mean and standard deviation of metrics over three independent runs.

**More qualitative results.** We present the qualitative comparison of the uncertainty methods on LF, LLFF, and RobustNeRF datasets in Figures 11 to 13, respectively. Additionally, we show the aleatoric and epistemic uncertainty maps of more scenes in the wild from Phototoursim [16] in Figure 14.

**Hyperparameter selection.** The regularization coefficient in the loss function is selected based on the quantitative metrics. Figure 9 illustrates how different coefficients affect image reconstruction and uncertainty estimation. In general, both excessively small and large coefficients lead to suboptimal performance, and the best hyperparameter value is inherently scene-dependent. The specific regularization coefficients utilized to produce the reported results are detailed in Table 3.

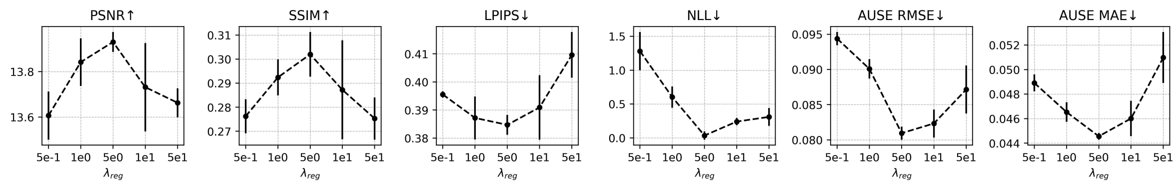


Figure 9. Sensitivity study of regularization coefficient's effect on all the quantitative metrics of *Leaves* scene.

| Scene | Africa | Basket | Statue | Torch | Fern | Flower | Fortress | Horns | Leaves | Orchids | Room | T-Rex | Android | Crab | Statue | Yoda |
|---|---|---|---|---|---|---|---|---|---|---|---|---|---|---|---|---|
| $\lambda_{\text{reg}}$ | 5e-3 | 1e-1 | 1e-3 | 1e0 | 1e0 | 5e-2 | 1e0 | 5e-1 | 5e0 | 1e0 | 5e-1 | 5e0 | 5e-3 | 5e-4 | 1e-4 | 1e-5 |

Table 3. The regularization coefficients used in each scene of LF, LLFF, and RobustNeRF datasets.

**Mutual causes of aleatoric and epistemic uncertainties.** Various complex elements in a 3D scene can lead to elevated levels of either aleatoric or epistemic uncertainty. However, attributing each specific factor exclusively to one type of uncertainty is often inappropriate, as many factors affect both uncertainties in different ways and to varying degrees. For example, transient objects increase AU due to color variations introduced by motion, while simultaneously raising EU through partial occlusions. Similarly, edges or high-frequency non-smooth regions tend to exhibit higher AU since their radiance is highly sensitive to input rays, as small inaccuracies in sensing, digitization, or poses can yield large radiance variations, resulting in nearly irreducible data uncertainty; meanwhile, the irregular geometry of such regions obstructs ray coverage and limits supervision signals from those surfaces, thereby increasing EU as well.

**Uncertainties of transients.** Transient objects can lead to both higher aleatoric and epistemic uncertainties. In practice, the uncertainties of the transient regions depend on the densities assigned to them by the model. Figure 10 shows ten images from two RobustNeRF scenes where the model is trained on images with cluttered objects. It can be observed that when the model cannot disambiguate the transients and the floaters appear in the test renderings, both AU and EU tend to be higher on them, meaning that the model simultaneously receives inconsistent radiance signals (high AU) and lacks sufficient knowledge to determine the presence or geometry of the transients (high EU). When the model resolves the transient objects (by minimizing their densities and removing them from volumetric rendering), the floaters disappear in the test image reconstructions and only AU remains high, indicating that the model no longer lacks the knowledge to determine the presence of the transients but still records the color inconsistency from the training signals as high AU.

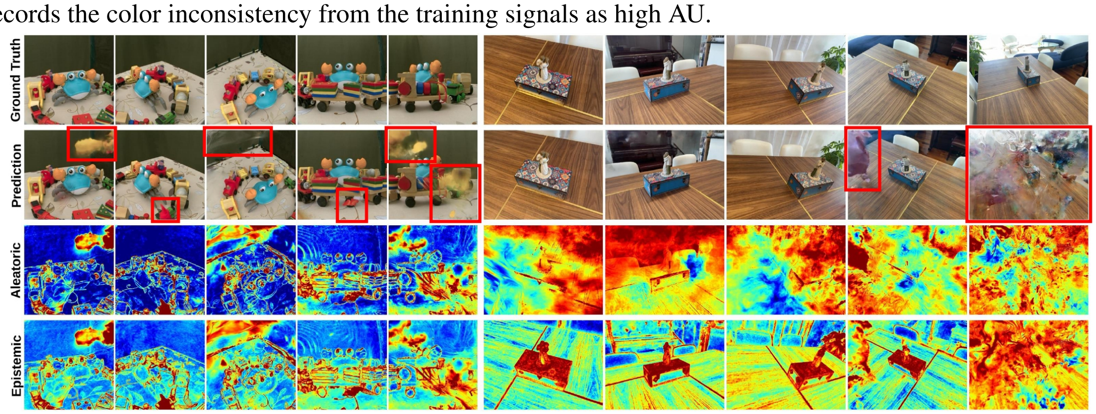


Figure 10. Aleatoric and epistemic uncertainties of scenes with transient objects. The red bounding boxes delineate the erroneous artifacts in test renderings caused by transients in the training views. If the model fails to suppress the floaters, both AU and EU are elevated on the transients; If the model resolves the transience, only AU is higher on the regions where the training transients were once present.

| Scene | Method | PSNR↑ | SSIM↑ | LPIPS↓ | NLL↓ | AUSE RMSE↓ | AUSE MAE↓ |
|---|---|---|---|---|---|---|---|
| Africa | Baseline | 26.5406 ±0.1903 | 0.9019 ±0.0009 | 0.0565 ±0.0010 | | | |
| | Dropout | 26.6798 ±0.0205 | 0.8986 ±0.0007 | 0.0590 ±0.0014 | 4.0201 ±0.2676 | 0.0148 ±0.0003 | 0.0064 ±0.0001 |
| | Normal | 27.4766 ±1.5843 | 0.9028 ±0.0192 | 0.0608 ±0.0210 | -1.4911 ±0.6587 | 0.0078 ±0.0023 | 0.0033 ±0.0004 |
| | MoL | 28.0663 ±0.6656 | 0.9023 ±0.0082 | 0.0614 ±0.0056 | -2.3375 ±0.0088 | 0.0069 ±0.0001 | 0.0035 ±0.0001 |
| | Ensembles | 27.0083 ±0.0652 | 0.9171 ±0.0003 | 0.0491 ±0.0006 | 0.0871 ±0.1899 | 0.0087 ±0.0005 | 0.0037 ±0.0001 |
| | DANE | 27.0083 ±0.0652 | 0.9171 ±0.0003 | 0.0491 ±0.0006 | -0.9581 ±0.1721 | 0.0139 ±0.0010 | 0.0059 ±0.0003 |
| | Evidential | 29.8826 ±0.0617 | 0.9331 ±0.0002 | 0.0340 ±0.0015 | -2.3643 ±0.0030 | 0.0054 ±0.0000 | 0.0028 ±0.0000 |
| Basket | Baseline | 28.0171 ±0.0703 | 0.9114 ±0.0019 | 0.0474 ±0.0008 | | | |
| | Dropout | 27.3038 ±0.0176 | 0.8897 ±0.0018 | 0.0610 ±0.0016 | 6.2637 ±0.3747 | 0.0155 ±0.0005 | 0.0054 ±0.0002 |
| | Normal | 27.9387 ±0.6029 | 0.9087 ±0.0097 | 0.0517 ±0.0044 | 5.5852 ±2.7302 | 0.0137 ±0.0033 | 0.0043 ±0.0013 |
| | MoL | 27.5847 ±0.2379 | 0.9044 ±0.0007 | 0.0692 ±0.0015 | -2.2614 ±0.0438 | 0.0125 ±0.0016 | 0.0036 ±0.0002 |
| | Ensembles | 28.9951 ±0.0715 | 0.9258 ±0.0011 | 0.0427 ±0.0004 | -0.8529 ±0.3663 | 0.0058 ±0.0002 | 0.0023 ±0.0001 |
| | DANE | 28.9951 ±0.0715 | 0.9258 ±0.0011 | 0.0427 ±0.0004 | -1.0245 ±0.3048 | 0.0087 ±0.0010 | 0.0034 ±0.0004 |
| | Evidential | 29.1442 ±0.1841 | 0.9263 ±0.0008 | 0.0369 ±0.0002 | -2.1757 ±0.0901 | 0.0098 ±0.0008 | 0.0033 ±0.0001 |
| Statue | Baseline | 32.8018 ±0.1611 | 0.9645 ±0.0007 | 0.0221 ±0.0007 | | | |
| | Dropout | 31.8005 ±0.0787 | 0.9525 ±0.0009 | 0.0377 ±0.0007 | -1.1505 ±0.0358 | 0.0057 ±0.0002 | 0.0031 ±0.0001 |
| | Normal | 28.8110 ±1.1896 | 0.9457 ±0.0036 | 0.0424 ±0.0033 | -1.9682 ±0.4526 | 0.0055 ±0.0010 | 0.0017 ±0.0001 |
| | MoL | 30.6262 ±0.5385 | 0.9469 ±0.0083 | 0.0545 ±0.0174 | -2.9409 ±0.0318 | 0.0030 ±0.0002 | 0.0016 ±0.0001 |
| | Ensembles | 33.7663 ±0.0662 | 0.9718 ±0.0001 | 0.0198 ±0.0000 | -1.9914 ±0.0994 | 0.0029 ±0.0001 | 0.0017 ±0.0000 |
| | DANE | 33.7663 ±0.0662 | 0.9718 ±0.0001 | 0.0198 ±0.0000 | -2.1733 ±0.0538 | 0.0034 ±0.0002 | 0.0020 ±0.0001 |
| | Evidential | 32.8506 ±0.2748 | 0.9661 ±0.0003 | 0.0221 ±0.0003 | -2.9793 ±0.0192 | 0.0031 ±0.0001 | 0.0014 ±0.0000 |
| Torch | Baseline | 26.8557 ±0.0802 | 0.8911 ±0.0010 | 0.0599 ±0.0014 | | | |
| | Dropout | 26.6709 ±0.0290 | 0.8835 ±0.0005 | 0.0698 ±0.0007 | 5.5346 ±0.4652 | 0.0139 ±0.0005 | 0.0046 ±0.0001 |
| | Normal | 27.7991 ±0.1333 | 0.9087 ±0.0019 | 0.0574 ±0.0015 | -0.3559 ±1.1275 | 0.0090 ±0.0022 | 0.0023 ±0.0002 |
| | MoL | 26.6030 ±0.1090 | 0.8845 ±0.0028 | 0.0838 ±0.0042 | -2.6173 ±0.0145 | 0.0112 ±0.0005 | 0.0028 ±0.0000 |
| | Ensembles | 27.7419 ±0.0417 | 0.9086 ±0.0004 | 0.0528 ±0.0002 | 4.0553 ±1.4211 | 0.0105 ±0.0006 | 0.0026 ±0.0001 |
| | DANE | 27.7419 ±0.0417 | 0.9086 ±0.0004 | 0.0528 ±0.0002 | 2.4292 ±0.9753 | 0.0144 ±0.0013 | 0.0044 ±0.0005 |
| | Evidential | 27.9943 ±0.1674 | 0.9126 ±0.0017 | 0.0507 ±0.0041 | -2.2771 ±0.1350 | 0.0096 ±0.0022 | 0.0025 ±0.0003 |

Table 4. Mean and standard deviation of quantitative metrics over three runs on LF.

| Scene | Method | PSNR↑ | SSIM↑ | LPIPS↓ | NLL↓ | AUSE RMSE↓ | AUSE MAE↓ |
|---|---|---|---|---|---|---|---|
| Fern | Baseline | 20.1069 ±0.1190 | 0.5685 ±0.0005 | 0.3617 ±0.0050 | | | |
| | Dropout | 19.1317 ±0.1808 | 0.5153 ±0.0059 | 0.4432 ±0.0060 | 46.5072 ±8.3738 | 0.0517 ±0.0016 | 0.0294 ±0.0020 |
| | Normal | 20.1763 ±0.3308 | 0.5905 ±0.0115 | 0.3273 ±0.0133 | 47.5151 ±1.6352 | 0.0349 ±0.0014 | 0.0193 ±0.0005 |
| | MoL | 18.2953 ±0.6532 | 0.5222 ±0.0298 | 0.4279 ±0.0406 | 1.3336 ±0.2902 | 0.0605 ±0.0157 | 0.0257 ±0.0078 |
| | Ensembles | 20.7328 ±0.0591 | 0.6134 ±0.0016 | 0.3462 ±0.0019 | 3.2024 ±0.4579 | 0.0297 ±0.0004 | 0.0148 ±0.0002 |
| | DANE | 20.7328 ±0.0591 | 0.6134 ±0.0016 | 0.3462 ±0.0019 | 2.6334 ±0.4099 | 0.0332 ±0.0002 | 0.0172 ±0.0001 |
| | Evidential | 20.8095 ±0.1119 | 0.6216 ±0.0074 | 0.3005 ±0.0077 | -0.4856 ±0.1133 | 0.0301 ±0.0009 | 0.0160 ±0.0007 |
| Flower | Baseline | 18.3456 ±0.0046 | 0.4792 ±0.0068 | 0.4230 ±0.0116 | | | |
| | Dropout | 18.6701 ±0.1790 | 0.4990 ±0.0089 | 0.3780 ±0.0057 | 54.1338 ±2.6904 | 0.0554 ±0.0012 | 0.0341 ±0.0012 |
| | Normal | 12.6188 ±4.7635 | 0.2205 ±0.1075 | 0.7529 ±0.2290 | 9.0113 ±6.3991 | 0.0732 ±0.0073 | 0.0590 ±0.0115 |
| | MoL | 18.6338 ±0.2226 | 0.5140 ±0.0055 | 0.3665 ±0.0141 | 1.4129 ±0.1601 | 0.0589 ±0.0023 | 0.0296 ±0.0012 |
| | Ensembles | 18.7711 ±0.0344 | 0.5204 ±0.0036 | 0.3993 ±0.0050 | 7.7562 ±0.2043 | 0.0370 ±0.0004 | 0.0173 ±0.0002 |
| | DANE | 18.7711 ±0.0344 | 0.5204 ±0.0036 | 0.3993 ±0.0050 | 7.7131 ±0.2053 | 0.0371 ±0.0004 | 0.0174 ±0.0002 |
| | Evidential | 19.2606 ±0.1150 | 0.5254 ±0.0126 | 0.3957 ±0.0208 | 2.4728 ±0.6069 | 0.0409 ±0.0022 | 0.0238 ±0.0015 |
| Fortress | Baseline | 18.3478 ±0.1598 | 0.3906 ±0.0033 | 0.5240 ±0.0069 | | | |
| | Dropout | 18.3708 ±0.5357 | 0.4063 ±0.0039 | 0.5204 ±0.0077 | 52.6142 ±9.0302 | 0.0518 ±0.0069 | 0.0278 ±0.0022 |
| | Normal | 18.3146 ±0.0871 | 0.4100 ±0.0106 | 0.5060 ±0.0427 | 62.8832 ±20.7391 | 0.0515 ±0.0036 | 0.0248 ±0.0027 |
| | MoL | 17.4740 ±0.1443 | 0.3779 ±0.0064 | 0.6090 ±0.0253 | 1.8754 ±0.5340 | 0.0645 ±0.0009 | 0.0280 ±0.0003 |
| | Ensembles | 18.8273 ±0.0496 | 0.4438 ±0.0015 | 0.4517 ±0.0023 | 7.5589 ±0.8103 | 0.0369 ±0.0014 | 0.0188 ±0.0003 |
| | DANE | 18.8273 ±0.0496 | 0.4438 ±0.0015 | 0.4517 ±0.0023 | 7.1596 ±0.8387 | 0.0377 ±0.0017 | 0.0195 ±0.0003 |
| | Evidential | 18.7310 ±0.0406 | 0.4264 ±0.0065 | 0.4878 ±0.0040 | 0.2943 ±0.1765 | 0.0404 ±0.0011 | 0.0208 ±0.0005 |
| Horns | Baseline | 15.7052 ±0.1371 | 0.4527 ±0.0105 | 0.4451 ±0.0111 | | | |
| | Dropout | 15.4649 ±0.2658 | 0.4296 ±0.0113 | 0.4729 ±0.0074 | 159.8088 ±22.3326 | 0.0919 ±0.0057 | 0.0482 ±0.0025 |
| | Normal | 13.4923 ±0.2916 | 0.2336 ±0.0089 | 0.6160 ±0.0096 | 22.6808 ±7.0886 | 0.1130 ±0.0047 | 0.0807 ±0.0083 |
| | MoL | 14.5633 ±0.1664 | 0.3638 ±0.0457 | 0.5691 ±0.0891 | 2.1617 ±0.2982 | 0.1101 ±0.0039 | 0.0505 ±0.0008 |
| | Ensembles | 15.9843 ±0.0172 | 0.5025 ±0.0033 | 0.4240 ±0.0045 | 22.0785 ±1.0690 | 0.0759 ±0.0013 | 0.0328 ±0.0005 |
| | DANE | 15.9843 ±0.0172 | 0.5025 ±0.0033 | 0.4240 ±0.0045 | 15.3955 ±1.4795 | 0.0750 ±0.0014 | 0.0330 ±0.0006 |
| | Evidential | 15.7596 ±0.1745 | 0.5034 ±0.0074 | 0.3878 ±0.0075 | 1.8495 ±0.1097 | 0.0941 ±0.0055 | 0.0403 ±0.0023 |

Table 5. Mean and standard deviation of quantitative metrics over three runs on LLFF.

| Scene | Method | PSNR↑ | SSIM↑ | LPIPS↓ | NLL↓ | AUSE RMSE↓ | AUSE MAE↓ |
|---|---|---|---|---|---|---|---|
| Leaves | Baseline | 13.6976 ±0.1464 | 0.2557 ±0.0155 | 0.4167 ±0.0066 | | | |
| | Dropout | 13.9549 ±0.2228 | 0.2423 ±0.0248 | 0.4235 ±0.0211 | 141.2669 ±12.2890 | 0.1072 ±0.0025 | 0.0618 ±0.0024 |
| | Normal | 13.3743 ±0.0707 | 0.2525 ±0.0111 | 0.4239 ±0.0075 | 104.3151 ±41.1687 | 0.1064 ±0.0013 | 0.0553 ±0.0009 |
| | MoL | 12.8939 ±0.1964 | 0.2408 ±0.0179 | 0.4276 ±0.0162 | 4.1014 ±0.2543 | 0.1266 ±0.0053 | 0.0674 ±0.0044 |
| | Ensembles | 14.2397 ±0.0569 | 0.2960 ±0.0069 | 0.4319 ±0.0047 | 12.3460 ±0.5912 | 0.0915 ±0.0010 | 0.0471 ±0.0007 |
| | DANE | 14.2397 ±0.0569 | 0.2960 ±0.0069 | 0.4319 ±0.0047 | 11.6017 ±0.1579 | 0.0928 ±0.0009 | 0.0482 ±0.0006 |
| | Evidential | 13.9301 ±0.0437 | 0.3020 ±0.0093 | 0.3847 ±0.0035 | 0.0349 ±0.0607 | 0.0809 ±0.0009 | 0.0446 ±0.0003 |
| Orchids | Baseline | 14.5292 ±0.0830 | 0.3036 ±0.0057 | 0.3916 ±0.0103 | | | |
| | Dropout | 13.3110 ±0.4149 | 0.2151 ±0.0202 | 0.4709 ±0.0100 | 123.9834 ±10.5705 | 0.1195 ±0.0056 | 0.0762 ±0.0037 |
| | Normal | 14.9466 ±0.1068 | 0.3189 ±0.0126 | 0.3911 ±0.0160 | 25.0742 ±5.0559 | 0.0754 ±0.0028 | 0.0424 ±0.0013 |
| | MoL | 13.8818 ±0.0307 | 0.3242 ±0.0031 | 0.3706 ±0.0047 | 2.4593 ±0.0292 | 0.1058 ±0.0045 | 0.0506 ±0.0021 |
| | Ensembles | 14.8488 ±0.1379 | 0.3250 ±0.0081 | 0.3953 ±0.0065 | 9.7556 ±0.8979 | 0.0753 ±0.0037 | 0.0409 ±0.0017 |
| | DANE | 14.8488 ±0.1379 | 0.3250 ±0.0081 | 0.3953 ±0.0065 | 9.4356 ±0.7865 | 0.0746 ±0.0034 | 0.0407 ±0.0016 |
| | Evidential | 14.7012 ±0.1548 | 0.3253 ±0.0090 | 0.3601 ±0.0103 | 0.5681 ±0.2424 | 0.0843 ±0.0041 | 0.0459 ±0.0017 |
| Room | Baseline | 19.7859 ±0.0325 | 0.7196 ±0.0037 | 0.3864 ±0.0088 | | | |
| | Dropout | 19.1522 ±0.0418 | 0.6704 ±0.0097 | 0.4536 ±0.0085 | 79.6637 ±8.4028 | 0.0637 ±0.0016 | 0.0342 ±0.0006 |
| | Normal | 19.8485 ±0.2959 | 0.6766 ±0.0384 | 0.4178 ±0.0630 | 111.9164 ±13.8320 | 0.0465 ±0.0013 | 0.0232 ±0.0020 |
| | MoL | 17.6348 ±0.7025 | 0.5337 ±0.0754 | 0.6094 ±0.0874 | 3.1864 ±0.4821 | 0.0651 ±0.0042 | 0.0295 ±0.0026 |
| | Ensembles | 19.9259 ±0.0347 | 0.7492 ±0.0003 | 0.3656 ±0.0006 | 15.8667 ±0.7134 | 0.0347 ±0.0006 | 0.0161 ±0.0004 |
| | DANE | 19.9259 ±0.0347 | 0.7492 ±0.0003 | 0.3656 ±0.0006 | 13.4646 ±0.4077 | 0.0368 ±0.0004 | 0.0174 ±0.0005 |
| | Evidential | 19.9548 ±0.0570 | 0.7172 ±0.0181 | 0.3660 ±0.0299 | 1.2947 ±1.1068 | 0.0465 ±0.0027 | 0.0221 ±0.0012 |
| T-Rex | Baseline | 19.7067 ±0.0095 | 0.6063 ±0.0041 | 0.3463 ±0.0047 | | | |
| | Dropout | 19.0824 ±0.1470 | 0.5750 ±0.0059 | 0.4119 ±0.0046 | 67.4407 ±5.4653 | 0.0525 ±0.0006 | 0.0290 ±0.0006 |
| | Normal | 19.6283 ±0.1296 | 0.6055 ±0.0176 | 0.3502 ±0.0238 | 59.4677 ±29.4200 | 0.0379 ±0.0026 | 0.0189 ±0.0008 |
| | MoL | 17.9974 ±0.5803 | 0.5127 ±0.0837 | 0.4935 ±0.1085 | 1.4452 ±0.3356 | 0.0594 ±0.0049 | 0.0255 ±0.0029 |
| | Ensembles | 20.0150 ±0.0311 | 0.6373 ±0.0019 | 0.3317 ±0.0028 | 10.7621 ±0.1102 | 0.0293 ±0.0004 | 0.0145 ±0.0002 |
| | DANE | 20.0150 ±0.0311 | 0.6373 ±0.0019 | 0.3317 ±0.0028 | 10.4152 ±0.0855 | 0.0295 ±0.0004 | 0.0146 ±0.0002 |
| | Evidential | 19.8874 ±0.0246 | 0.6329 ±0.0048 | 0.3177 ±0.0095 | -0.6168 ±0.0407 | 0.0455 ±0.0004 | 0.0226 ±0.0006 |

Table 6. Mean and standard deviation of quantitative metrics over three runs on LLFF.

| Scene | Method | PSNR↑ | SSIM↑ | LPIPS↓ | NLL↓ | AUSE RMSE↓ | AUSE MAE↓ |
|---|---|---|---|---|---|---|---|
| Android | Baseline | 22.8865 ±0.0476 | 0.7691 ±0.0008 | 0.1545 ±0.0011 | | | |
| | Dropout | 22.6094 ±0.0779 | 0.7552 ±0.0001 | 0.1699 ±0.0009 | 17.8212 ±0.1534 | 0.0308 ±0.0002 | 0.0188 ±0.0001 |
| | Normal | 23.9819 ±0.0770 | 0.8146 ±0.0013 | 0.1058 ±0.0021 | 4.9525 ±0.7433 | 0.0227 ±0.0006 | 0.0152 ±0.0003 |
| | MoL | 22.1825 ±0.0186 | 0.7395 ±0.0002 | 0.1905 ±0.0008 | -0.7117 ±0.0656 | 0.0273 ±0.0006 | 0.0172 ±0.0005 |
| | Ensembles | 23.4866 ±0.0304 | 0.8012 ±0.0006 | 0.1381 ±0.0006 | 8.1690 ±0.8485 | 0.0265 ±0.0001 | 0.0158 ±0.0000 |
| | DANE | 23.4866 ±0.0304 | 0.8012 ±0.0006 | 0.1381 ±0.0006 | 7.4801 ±0.8655 | 0.0274 ±0.0001 | 0.0164 ±0.0000 |
| | Evidential | 23.8915 ±0.0651 | 0.8116 ±0.0034 | 0.1047 ±0.0007 | -1.1616 ±0.0266 | 0.0231 ±0.0003 | 0.0153 ±0.0002 |
| Crab | Baseline | 28.6708 ±0.2399 | 0.9034 ±0.0038 | 0.1124 ±0.0072 | | | |
| | Dropout | 27.5569 ±0.3792 | 0.8850 ±0.0049 | 0.1186 ±0.0065 | 24.1365 ±2.5685 | 0.0216 ±0.0012 | 0.0074 ±0.0007 |
| | Normal | 27.7154 ±0.2508 | 0.9062 ±0.0016 | 0.0971 ±0.0025 | 2.9771 ±1.6485 | 0.0151 ±0.0007 | 0.0062 ±0.0004 |
| | MoL | 27.0696 ±0.2685 | 0.8767 ±0.0044 | 0.1374 ±0.0061 | -2.5692 ±0.0274 | 0.0186 ±0.0013 | 0.0065 ±0.0005 |
| | Ensembles | 30.0907 ±0.0696 | 0.9206 ±0.0007 | 0.1072 ±0.0006 | -0.3212 ±0.4515 | 0.0048 ±0.0005 | 0.0021 ±0.0001 |
| | DANE | 30.0907 ±0.0696 | 0.9206 ±0.0007 | 0.1072 ±0.0006 | -0.0123 ±0.2259 | 0.0234 ±0.0006 | 0.0101 ±0.0000 |
| | Evidential | 29.9324 ±0.0145 | 0.9160 ±0.0086 | 0.0795 ±0.0154 | -2.0303 ±0.2399 | 0.0150 ±0.0059 | 0.0084 ±0.0058 |
| Statue | Baseline | 20.1787 ±0.0379 | 0.7489 ±0.0046 | 0.2356 ±0.0072 | | | |
| | Dropout | 20.0340 ±0.0841 | 0.7213 ±0.0068 | 0.2772 ±0.0159 | 35.4746 ±2.1971 | 0.0464 ±0.0013 | 0.0304 ±0.0008 |
| | Normal | 20.1453 ±0.0154 | 0.7780 ±0.0039 | 0.2128 ±0.0061 | 17.9184 ±2.0826 | 0.0413 ±0.0008 | 0.0275 ±0.0007 |
| | MoL | 19.3304 ±0.1637 | 0.6834 ±0.0032 | 0.3300 ±0.0069 | 0.0773 ±0.0274 | 0.0571 ±0.0005 | 0.0380 ±0.0007 |
| | Ensembles | 20.5674 ±0.0059 | 0.7843 ±0.0008 | 0.2166 ±0.0028 | 9.9047 ±0.3519 | 0.0297 ±0.0003 | 0.0191 ±0.0001 |
| | DANE | 20.5674 ±0.0059 | 0.7843 ±0.0008 | 0.2166 ±0.0028 | 8.4305 ±0.2763 | 0.0367 ±0.0002 | 0.0235 ±0.0000 |
| | Evidential | 20.8284 ±0.0496 | 0.8017 ±0.0010 | 0.1780 ±0.0019 | -0.0313 ±0.3149 | 0.0362 ±0.0008 | 0.0243 ±0.0004 |
| Yoda | Baseline | 29.1458 ±0.4079 | 0.8969 ±0.0081 | 0.1284 ±0.0118 | | | |
| | Dropout | 28.8770 ±0.1990 | 0.8857 ±0.0041 | 0.1322 ±0.0020 | 14.0873 ±5.1782 | 0.0148 ±0.0034 | 0.0073 ±0.0014 |
| | Normal | 29.3523 ±0.5839 | 0.9099 ±0.0040 | 0.1088 ±0.0043 | 16.1012 ±8.0429 | 0.0209 ±0.0034 | 0.0115 ±0.0018 |
| | MoL | 26.5671 ±0.3613 | 0.8688 ±0.0051 | 0.1617 ±0.0070 | -2.3751 ±0.0676 | 0.0186 ±0.0018 | 0.0088 ±0.0010 |
| | Ensembles | 30.6364 ±0.1516 | 0.9188 ±0.0025 | 0.1135 ±0.0029 | 0.7713 ±0.1332 | 0.0044 ±0.0001 | 0.0020 ±0.0001 |
| | DANE | 30.6364 ±0.1516 | 0.9188 ±0.0025 | 0.1135 ±0.0029 | 0.5383 ±0.2742 | 0.0257 ±0.0015 | 0.0116 ±0.0006 |
| | Evidential | 30.2646 ±0.1857 | 0.9272 ±0.0065 | 0.0826 ±0.0124 | -1.8577 ±0.2073 | 0.0139 ±0.0009 | 0.0072 ±0.0012 |

Table 7. Mean and standard deviation of quantitative metrics over three runs on RobustNeRF.

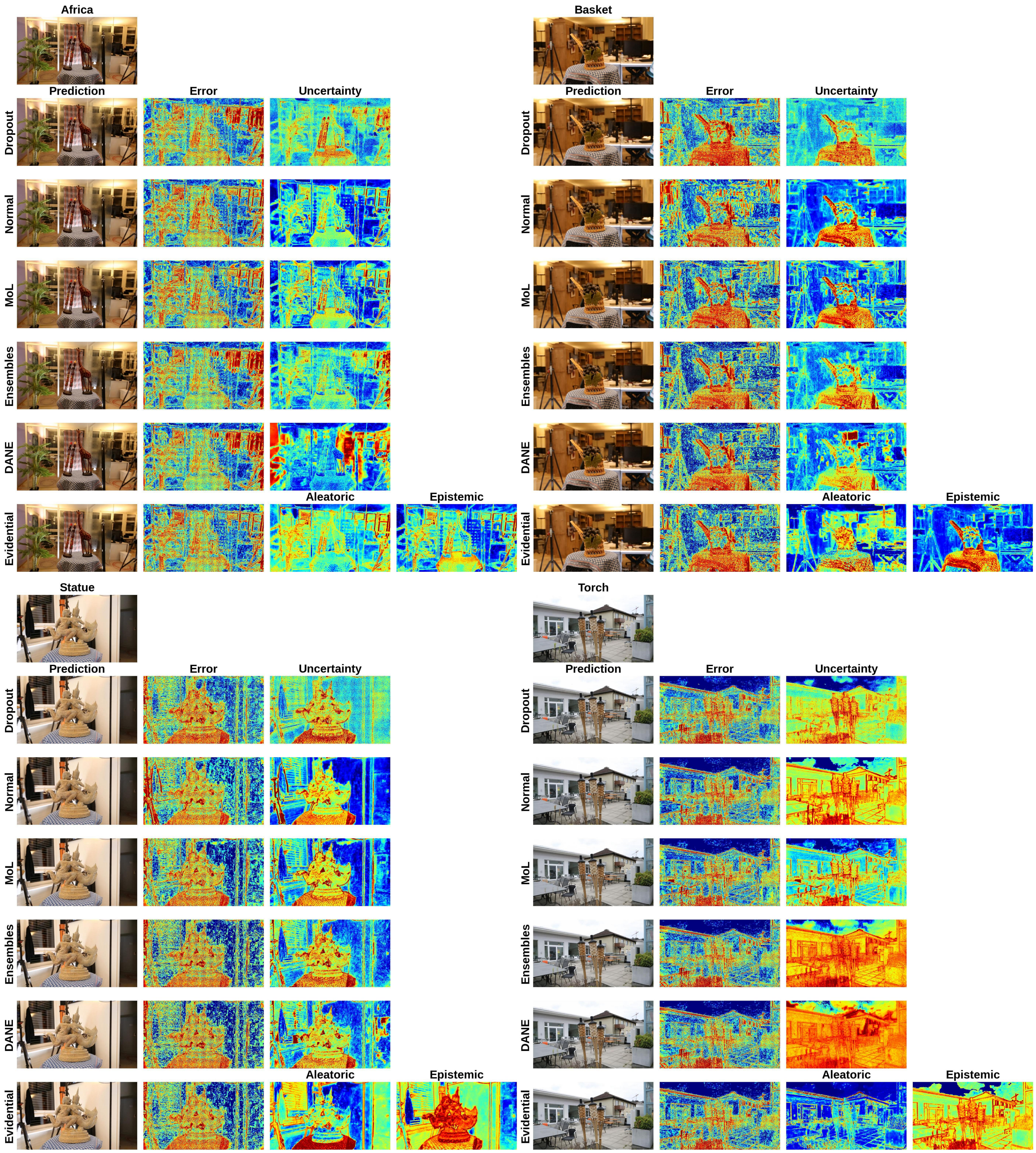


Figure 11. Qualitative comparison on LF.

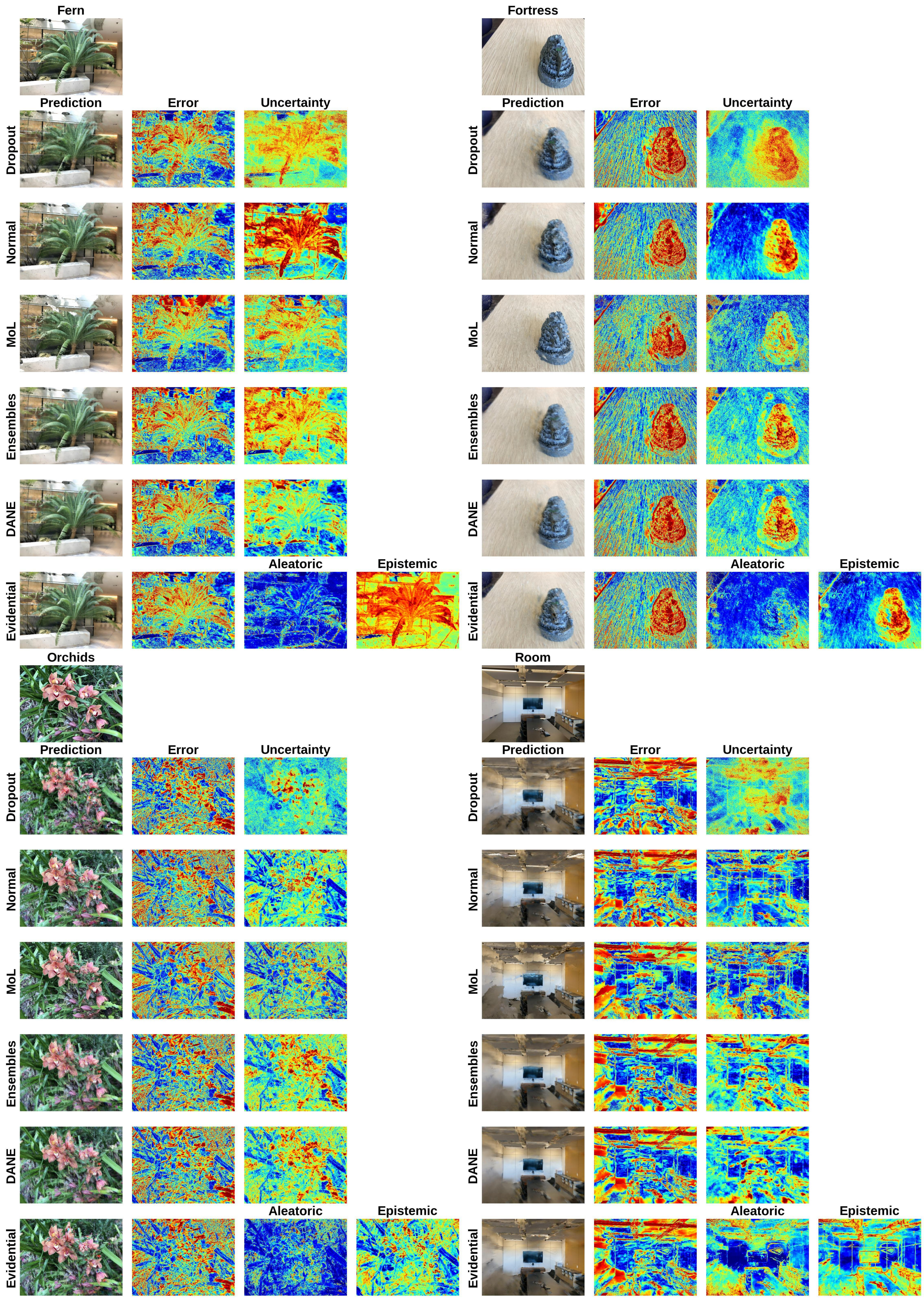


Figure 12. Qualitative comparison on LLFF.

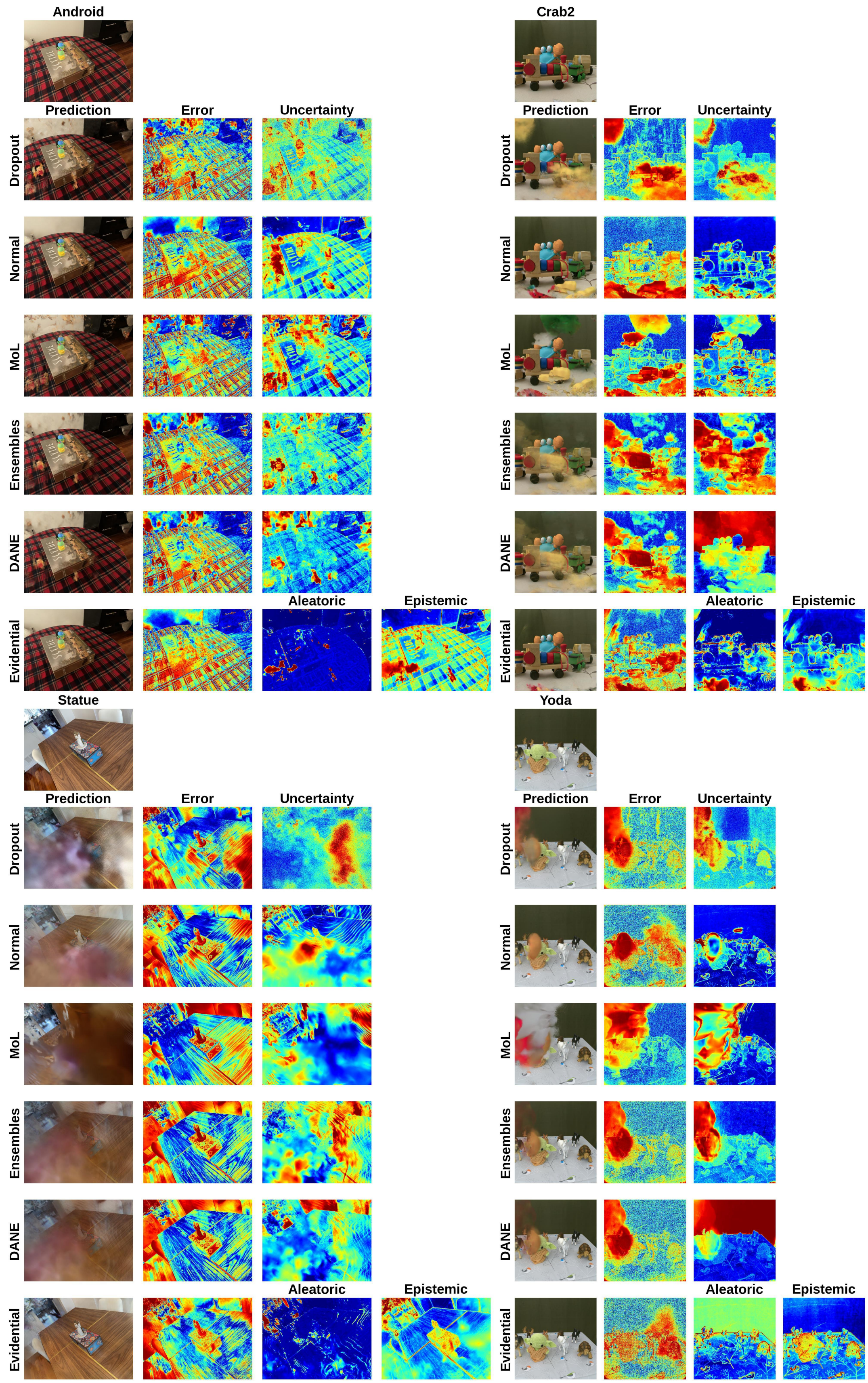


Figure 13. Qualitative comparison on RobustNeRF.

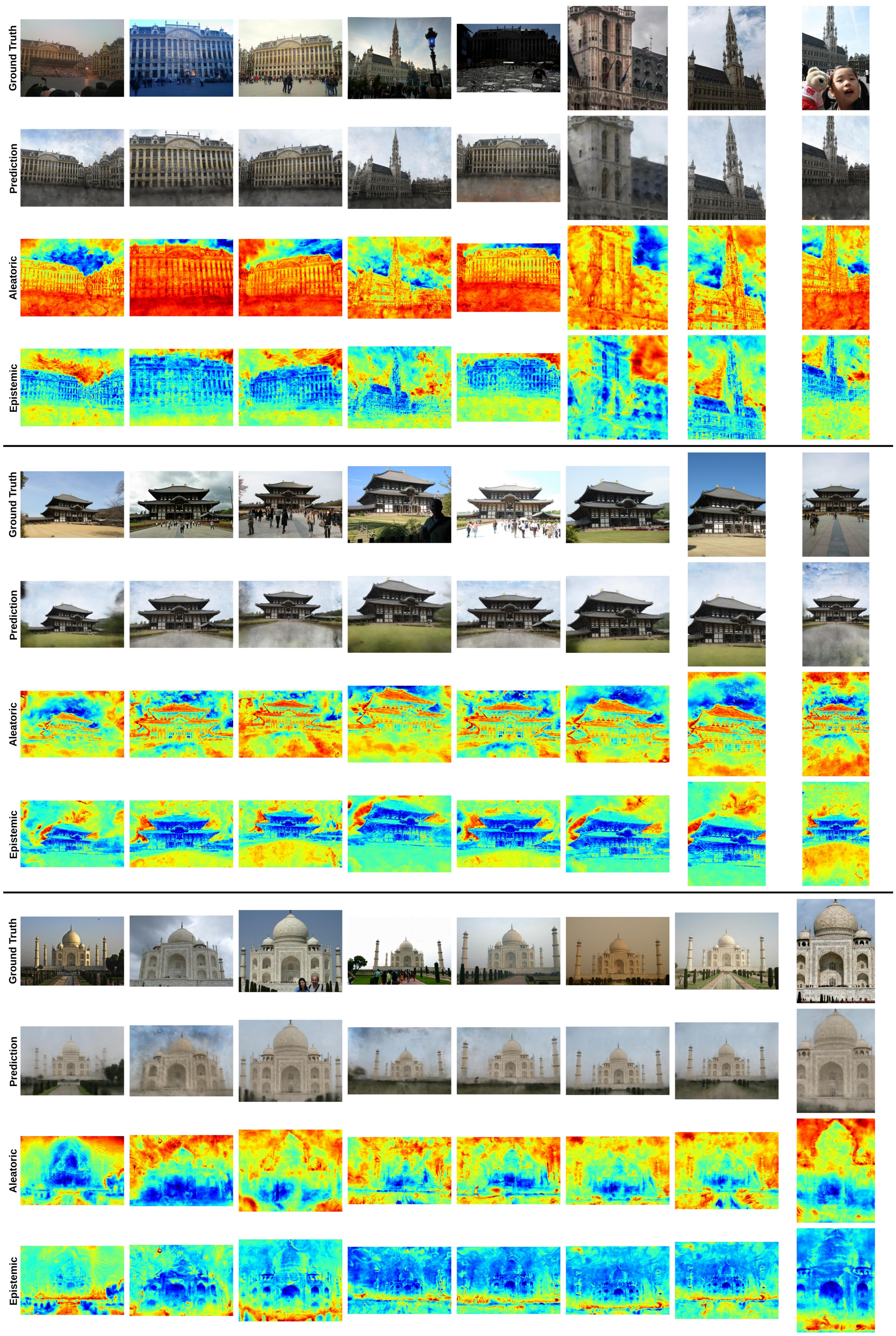


Figure 14. Aleatoric and epistemic uncertainty maps for three in-the-wild scenes from Phototourism. Aleatoric uncertainty peaks in regions with high radiance variance (e.g., sky higher above, building facades, moving figures), whereas epistemic uncertainty is concentrated in areas frequently occluded (e.g., sky directly behind the buildings or objects obscured by pedestrians).